Highlights

- Myoma-based ECM models are suitable for *in vitro* chemoradiation assays.
- Blocking of HPSE1 activity combined with IR may induce tongue cancer cell invasion.
- Low doses of IR may increase MMP expression and invasion in tongue cancer cells.

Effects of ionizing radiation and HPSE1 inhibition on the invasion of oral tongue carcinoma cells on human extracellular matrices *in vitro*

Otto Väyrynen[a, b], Markku Piippo[a, b], Hannaleena Jämsä[a, b], Tuomas Väisänen[a, b], Carlos E. B. de Almeida[c], Tuula Salo[a, b, d, e], Sotiris Missailidis[f] and Maija Risteli[a, b]

[a]Cancer Research and Translational Medicine Research Unit, Faculty of Medicine, University of Oulu, Oulu, Finland

[b]Medical Research Center Oulu, Oulu University Hospital, University of Oulu, Oulu, Finland

[c]Laboratório de Radiobiologia, Instituto de Radioproteção e Dosimetria, Comissão Nacional de Energia Nuclear, Rio de Janeiro, Brazil

[d]Department of Oral and Maxillofacial Diseases, University of Helsinki, Helsinki, Finland

[e]HUSLAB, Department of Pathology, Helsinki University Central Hospital, University of Helsinki, Helsinki, Finland

[f]Bio-Manguinhos Institute of Technology in Immunobiologics, FIOCRUZ, Rio de Janeiro, Brazil

Running title: Ionizing radiation and human extracellular matrices in carcinoma invasion

Correspondence: Maija Risteli, Cancer Research and Translational Medicine Research Unit, Faculty of Medicine, University of Oulu, P.O. Box 8000, FI-90014 University of Oulu, Finland. Tel.: +358 294 48 0000, E-mail: maija.risteli@oulu.fi

Keywords: oral tongue cancer, ionizing radiation, aptamer, Myogel, HPSE1

ABSTRACT

Chemoradiation is an established approach in the treatment of advanced oral tongue squamous cell carcinoma (OTSCC), but therapy may cause severe side-effects due to signal interchanges between carcinoma and the tumour microenvironment (TME). In this study, we examined the potential use of our human 3D myoma disc and Myogel models in *in vitro* chemoradiation studies by analysing the effects of ionizing radiation (IR) and the combined effect of heparanase I (HPSE1) inhibitors and IR on OTSCC cell proliferation, invasion and MMP-2 and -9 production. Finally, we analysed the long-term effects of IR by studying clones of previously irradiated and invaded HSC-3 cells. We found that in both human uterine leiomyoma-based extracellular matrix models IR inhibited the invasion of HSC-3 cells, but blocking HPSE1 activity combined with IR induced their invasion. Low doses of IR increased MMP expression and initiated epithelial-mesenchymal transition in cells cultured on myoma discs. We conclude that myoma models offer consistent methods for testing human carcinoma cell invasion and phenotypic changes during chemoradiation treatment. In addition, we showed that IR had long-term effects on MMP-2 and -9, which might elicit different HSC-3 invasion responses when cells were under the challenge of HPSE1 inhibitors and IR.

INTRODUCTION

Squamous cell carcinoma (SCC) is the most common cancer in the oral cavity [1], and most of the tumours occur along the lateral borders of the oral tongue (OT) [2], [3]. Despite advances in diagnostics and therapeutics, the survival rate of oral tongue squamous cell carcinoma (OTSCC) has improved by only 5% in the past 20 years, and in general the 5- year survival rate remains around 60% [4].

Treatment approaches for tongue cancer include surgery, in advanced stages combined with radiotherapy and sometimes chemotherapy. Although radiotherapy has proven its benefit in several

clinical studies, some patients develop local recurrences and metastases after the treatment. *In vitro* studies have shown that ionizing radiation (IR) increases cell migration and/or invasion due to increased expression of pro-migratory factors and the epithelial-mesenchymal transition (EMT) of cancer cells. Furthermore, cells in the irradiated tumour microenvironment (TME) may support the invasiveness of cancer cells [5], [6]. OTSCC is often refractory and there are only a few drugs for the treatment of advanced cancer. Currently, an established standard for first-line treatment of recurrent metastatic head and neck squamous cell carcinomas (HNSCCs), including OTSCC, is a combination of cisplatin/carboplatin, 5-fluorouracil (5-FU) and a EGFR–directed monoclonal antibody, Erbitux (cetuximab) [7]–[9]. In 2016, the US Food and Drug Administration (FDA) approved the use of two immune checkpoint inhibitors (ICIs), nivolumab and pembrolizum, in the treatment on HNSCC for some patients [10], [11].

We have introduced a human 3D myoma disc organotypic model [12], [13] and a gelatinous leiomyoma matrix, Myogel, for *in vitro* human cell invasion experiments [14], [15]. The hypoxic myoma discs mimic the TME of solid human tumours, and they contain a variety of non-vital cells and soluble invasion-related factors such as lysyl oxidase [16]. Recently, we showed that the invasion efficiency of the OTSCC cells into myoma depends on the amount of tenascin-C and soluble growth factors and their receptors in the tissue discs [17]. Myogel, on the other hand, provides a soluble human TME matrix for cancer studies. Compared with the commercial mouse tumour-derived matrix Matrigel®, Myogel contains e.g. latent and active MMP-2, tenascin-C and collagen types XII and XIV, which are not present in Matrigel® [14]. A metastatic niche is required for the survival and growth of metastasizing cancer cells [18]–[21]. Formation of this niche is associated with the deposition and remodelling of extracellular matrix (ECM) and the presence of hypoxia, growth factors, cytokines and chemokines [22]–[24]. Interestingly, since the composition

of myoma tissue shares the characteristics of the metastatic niche [14], [16] myoma models enable preclinical drug and chemoradiation testing.

The patient´s response to chemoradiotherapy depends greatly on the characteristics of the cancer. Therefore, new methods for treatment testing are needed in order to design personalized therapies. In this study, we tested the usability and consistency of human TME-mimicking tissue methods for analysing the effects of chemoradiation using commercial OTSCC cell lines. We have previously studied the feasibility of anti-heparanase aptamers as therapeutic agents against OTSCC with myoma discs [25], and now we further explored the effectiveness of these aptamers together with IR in a myoma disc model and in Myogel. We investigated also the effects of anti-heparanase 1 (HPSE1) antibody, which inhibits heparanase activity [26], and cetuximab (Erbitux), an EGFR inhibitor [27]. Furthermore, we assessed the short- and long-term effects of IR and invasion on OTSCC cell lines in myoma organotypic culture and on plastic.

MATERIALS AND METHODS

Cell culture and irradiation

Human tongue squamous cell carcinoma cell lines HSC-3 (JCRB 0623; Osaka National Institute of Health Sciences), SCC-25 (ATCC, CRL 1628) and SAS (JCRB-0260, Osaka National Institute of Health Sciences) were cultured in 1:1 Dulbecco's Modified Eagle Medium (DMEM)/Ham's Nutrient Mixture F-12 (Gibco) supplemented with 10% heat-inactivated foetal bovine serum (FBS) (Gibco), 100 U/ml penicillin, 100 µg/ml streptomycin, 50 µg/ml ascorbic acid, 250 ng/ml Amphotericin B and 0.4 µg/ml hydrocortisone (all from Sigma-Aldrich). All cell lines were cultured at 37°C in a humidified atmosphere of 95% air and 5% CO_2 and passaged routinely using trypsin-EDTA (Sigma-Aldrich).

Cell cultures in different experiments were irradiated at doses of 2, 4 and 8 Gy with a Varian Clinac iX linear accelerator (15 MV photon beam) at a dose rate of 4 Gy/min and a field size of 30 cm*30 cm in the Radiotherapy Unit of Oulu University Hospital. For comparison, an unirradiated control group (0 Gy) was included in each experiment. Cells were treated with 0.7 mM/10 µg/ml of an antibody against heparanase (Anti-HPSE1) [26], 1 µM 1.5 M short protected heparanase aptamer (inverted 3'-base dT5) [28] and 10 µg/ml of Erbitux (Merck Serono).

Irradiated and invaded HSC-3 cell clones were established from the bottom of the two wells of a single 24-well Transwell invasion experiment (see later). Cells were cultured 4-10 passages after irradiation, and in each experiment 0, 2, 4 and 8 Gy clones had equal passage numbers.

Myoma disc organotypic culture

Uterine leiomyoma tissues were obtained from routine surgeries of otherwise healthy donors after informed consent. The study was reviewed by the Regional Ethics Committee of the Northern Ostrobothnia Hospital District (license number 35/2014). HSC-3 cells (700 000 cells) were added on myoma discs in duplicates and cultured in normal culture medium containing the indicated concentrations of drugs for 12 days, during which the media and drugs were changed every 3 days [12], [13]. After this, the samples were irradiated as described above. Finally, all samples were incubated in culture media for 6 days in order to visualize the possible IR-induced cell invasion in the organotypic myoma model. At day 18, one of the myoma cultures was fixed in Zinc fixative, dehydrated, bisected and embedded in paraffin. The other myoma culture was frozen and embedded with Tissue Tek® OCT™ (Sakura).

Immunohistochemistry and quantification of invasion, proliferation, MMPs and EMT

The paraffinized irradiated myoma blocks were sliced in 6 µm sections with a microtome. The slices were deparaffinized and hydrated in graded alcohol solutions to deionized water. The activity of endogenous peroxidase was blocked with 0.3% H_2O_2 in methanol for 30 min as the specimens were prepared for immunohistochemistry of cytokeratin AE1/AE3, Ki-67, E-cadherin, vimentin, HPSE1, MMP-2 and MMP-9 antibodies. The information of the primary antibodies is shown in Table S1. The antigen retrieval was conducted by microwaving (T/T Mega) the specimens in REAL Target Retrieval Solution, pH 6 (citrate buffer) (Dako) or in 10 mM Tris/1 mM EDTA, pH 9 for 20 min. Sections were blocked with normal serum (Vector Laboratories) in 2% bovine serum albumin/phosphate-buffered saline (BSA/PBS) for 30 min and incubated with primary antibodies in an incubator chamber (37°C) for another 30 min and finally overnight at 4°C. Antibody dilutions were prepared in REAL Antibody Diluent (Dako). Biotinylated secondary antibody of appropriate species (Vector Laboratories) was applied for 60 min, and StreptABComplex/HRP (Dako) in 0.5 M NaCl/PBS was applied for 30 min. After each step, the sections were washed twice in PBS for 10 min. The antigen was then visualized by using 3,3′-diaminobenzidine (DAB, brown; Vector Laboratories) for 3 min. DAB-stained sections were counterstained with Mayer's haematoxylin and mounted with xylene. For negative controls, normal serum or IgG of appropriate species (Dako) was used instead of primary antibody.

Images were acquired from the sections with a DMRB photo microscope connected to a DFC-480 camera using QWin V3 software (all from Leica Microsystems). The invasion area and invasion depth were measured from the pancytokeratin-stained histological sections with Fiji software as previously described [12], [13]. Altogether 24 measurements per test were obtained. Cell proliferation rate was quantified as a percentage of Ki-67-positive carcinoma cells among all carcinoma cells per microscopic field at 200 x magnification. Six fields per myoma sample were

analysed. To evaluate the possible epithelial-mesenchymal transition of carcinoma cells, 6 hotspot images with 400 x magnification were acquired for each sample. For vimentin and HPSE1, the scoring was assessed by counting the percentage of positive cells/total cells. With E-cadherin, the intensity of staining was scored with a scale of 0-3 (0= no staining, 1=low, 2=moderate, 3=high intensity) from both the surface area and the invasion area. For MMP-2 and -9, hotspot images with 200 x magnification were acquired for the un-irradiated samples and for the samples irradiated with the highest dose (8 Gy).

Invasion assay

The filter of the Transwell-24 plate, pore size 8 μm (Corning) was coated with 50 μl of Myogel extracellular matrix developed in our laboratory (2.4 mg/ml of protein, 0.2% agarose in serum free culture medium) [14], [15] and incubated at room temperature (RT) for 30 min. Next, 500 μl of normal medium containing the indicated amount of drugs was added in the bottom chambers. Altogether 50000-70000 cells were seeded into the upper chambers in a 200 μl medium, in which FBS was replaced by 0.5% lactalbumin (Sigma-Aldrich) and contained the indicated amount of drugs. The cells were allowed to grow for 21 h, after which the cells were irradiated as described above. Drugs were changed in the wells of all plates. For irradiated and invaded cells, only normal and lactalbumin culture media were used in the assay. Cells were allowed to invade for 72 h and were then fixed in 4% neutral-buffered Formalin for 1 h and washed once with PBS. Cells were stained with 1% Toluidine blue-1% Borax for 10 min at RT and washed several times with distilled water. Then, non-invaded cells on the upper surface of the filter were carefully removed with a wet cotton swab. Toluidine blue stain was eluted with 1% SDS and absorbance was measured at 650 nm using a Victor2 Microplate Reader (Perkin Elmer Wallac) [14]. Results represent the average of three to five independent experiments, performed in triplicate.

Proliferation assay

The irradiated and invaded HSC-3 cells were seeded in normal media on 96-well culture plates at a density of 5000 cells/well in quadruplicate. The cell proliferation was determined after 24, 48 and 72 h using the Cell Proliferation ELISA BrdU (Roche) according to the manufacturer's protocol. Absorbance was measured at 450 nm using a Victor2 Microplate Reader (Perkin Elmer Wallac). Media-only-containing wells were measured as a blank control. The results represent the average of three separate experiments.

Clonogenic assay

For analysis of irradiated and invaded HSC-3 cells, 750 or 500 cells were seeded on a 6-well plate in triplicate and 150 or 100 cells on a 24-well plate in quadruplicate. For drug treatments, HSC-3 cells were seeded in normal media on a 24-well culture plate at a density of 150-600 (0-8 Gy)/well in quadruplicate. The cells were allowed to attach 6 h, after which the drugs were added at the indicated concentrations. The next morning, the cells were irradiated as described above. Drugs/medium were changed after 3 days. Cells were cultured 7 days, fixed with formalin and stained with crystal violet. The results represent the average of three separate experiments, and the clonogenic viability of the cells was calculated as previously described [29].

Immunoblot analysis

The confluent cell flasks were washed twice with PBS and cells were homogenized with 50 mM Tris-HCl pH 7.5, 10 mM $CaCl_2$, 150 mM NaCl, 0.05% (v/v) Brij-35 (Sigma-Aldrich) buffer including Complete mini EDTA-free protease inhibitor cocktail (Roche). For analysis of signalling protein phosphorylation, cells were serum-starved for 24 h and treated with normal cell culture

medium for 1 h. Cells were homogenized with buffer as above, which also contained PhosSTOP™ phosphatase inhibitor tablet (Roche). The cell debris was removed by centrifugation. The protein concentrations were measured with DC Protein assay (Bio-Rad), and 20 or 50 µg of soluble proteins were separated under reducing conditions by 8% or 12% SDS-PAGE gels and transferred to an Immobilon-P membrane (Millipore). The membranes were blocked with 5% milk powder or for phospho-antibodies 5% BSA in Tris-buffered saline –0.1% Tween 20 and incubated overnight with mouse anti-E-cadherin (Invitrogen), monoclonal mouse anti-vimentin (Dako), anti-heparanase 1 (Abcam), HPA1 (Santa Cruz Biotechnology), EGF receptor, Phospho-EGF receptor (Tyr1068), p44/42 MAPK (Erk1/2), Phospho-p44/42 MAPK (Erk1/2) (Thr202/Tyr204), Akt, Phospho-Akt (Ser473) antibodies (all from Cell Signaling Technology) or anti-beta actin (Abcam) followed by a biotinylated anti-rabbit IgG (DAKO) or anti-mouse IgG (DAKO) and Vectastain ABC kit (Vector Laboratories). Immunocomplexes were visualized using a Pierce ECL Western blotting substrate (Thermo Scientific) and Luminescent image analyzer LAS-3000 (Fujifilm). Quantification of protein levels was performed with Fiji software and ß-actin was used to normalize the results. The results represent the average of two to four independent experiments, separated two to three times on SDS-PAGE gels.

Zymography and gelatinase assay

Cells were cultured in 70% confluency in 75 cm^2 flasks, washed with PBS, and Opti-MEM (Gibco) was added. Conditioned medium was collected 24 h later. Next, 75 µl of conditioned medium was concentrated with a speed-vac device, and samples were analysed with gelatin zymography in 10% SDS-PAGE, casted in the presence of 1 mg/ml fluorescently labelled gelatin (2-methoxy-2,4-diphenyl-3-[2H] furanone; Fluka). After electrophoresis, SDS was removed by 2.5% Triton X-100 to renature the gelatinases and gels were incubated in 50 mM Tris-HCl buffer, pH 7.8, 150 mM NaCl, 5 mM $CaCl_2$, 1 µM $ZnCl_2$ overnight at 37°C. The degradation of fluorescent gelatin was

visualized using Molecular imager ChemiDoc XRS+ (Bio-Rad) [30]. The intensities of bands were quantified with Fiji software. The results represent the average of three separate sample sets, each analysed two to four times. The band intensities were normalized to the cellular soluble protein concentration.

Gelatinase activity of 70 µl of conditioned medium was assayed with EnzChek® Gelatinase Assay Kit (Molecular Probes). DQ gelatin (Molecular Probes) was used with a final substrate concentration of 50 µg/ml. Otherwise, the assay was performed according to the manufacturer's protocol. The fluorescence was measured after 3 h incubation at 485/535 nm using a Victor2 Microplate Reader (Perkin Elmer Wallac). The results represent the average of three separate sample sets, each analysed three times. The fluorescence intensities were normalized to the cellular soluble protein concentration.

Statistical analysis

Calculations were performed with IBM SPSS Statistics version 22 (SPSS, Inc.). Depending on data distribution, the paired samples Student's T-test and Mann-Whitney U-test were mainly used to determine the statistical differences. In a few cases in which the distribution was skewed, the Wilcoxon non-parametric signed-rank test was used.

RESULTS

Ionizing radiation inhibits HSC3 cell invasion, and addition of an HPSE1 inhibitor restores this effect in a 3D myoma organotypic model

We have introduced a human 3D myoma organotypic disc model [12], [15] for *in vitro* invasion experiments. Previously, we showed that anti-heparanase aptamers inhibited the invasion of a highly aggressive OTSCC cell line, HSC-3, in myoma discs [25]. In this study, we analysed the

combined effect of aptamers and ionizing radiation (IR) on HSC-3 cell invasion. Cells with an antibody against heparanase (anti-HPSE1) and the anti-heparanase aptamer 1.5 M short protected (inverted 3'-base dT5) were first cultured for 12 days, after which myomas were irradiated and further cultured for 6 days. The cell invasion area (Fig. 1A) and invasion depth (Fig. 1B) were measured from the pancytokeratin AE1/AE3 antibody-stained histological sections. Irradiation alone significantly reduced the invasion area with a dose of 4 Gy (Fig. 1A) and the invasion depth with doses of 2 and 4 Gy (Fig. 1B). However, both values increased with a dose of 8 Gy with respect to the decrease observed with 4 Gy. Treatment with anti-HPSE1 and 1.5 M short protected aptamer significantly decreased the invasion area and invasion depth compared with untreated non-irradiated myomas. This is in accordance with our previous data showing the effect of these heparanase inhibitors on invasion [25]. Invasion depth of aptamer-treated cells decreased with an irradiation dose of 2 Gy compared with treated non-irradiated cells. Interestingly, the irradiation increased the invasion area and depth at doses of 4 and 8 Gy, respectively, when the samples were treated with anti-HPSE1 and 1.5 short protected aptamers. Our data suggest that blocking of HPSE1 activity combined with IR may induce cell invasion.

Myogel studies confirm the effect of ionizing radiation combined with an HPSE1 inhibitor on the invasion of OTSCC cells

We have previously introduced a human gelatinous leiomyoma matrix named Myogel [14] for *in vitro* invasion experiments [15]. We evaluated whether Myogel would be feasible to use in testing chemoradiation and whether the results would be comparable to the myoma disc model. To assess the differences between the two myoma-based invasion assays and to evaluate the effect of ionizing radiation in the presence and absence of HPSE1 inhibitors, we used HSC-3 [31], [32], SCC-25 [33] and SAS [34] OTSCC cell lines as models of more and less invasive OTSCC cell lines. We also included as a control EGFR antibody Erbitux treatment in addition to anti-HPSE1 antibody and 1.5

M short protected aptamer in a Transwell invasion assay combined with irradiation (Fig. 2). In the HSC-3 cell line, irradiation alone had only a slight diminishing effect on invasion (Fig. 2A). The treatments alone seemed to reduce the invasion compared with untreated, non-irradiated cells. Interestingly, increasing irradiation dose appeared to induce cell invasion of treated cells compared with the corresponding non-irradiated cells, but this was the case only with the highly invasive HSC-3 cell line. This effect was not confirmed in poorly invasive SCC-25 or in SAS cell lines.

In a less invasive cell line, SCC-25, the irradiation alone significantly decreased the invasion with doses of 4 and 8 Gy (Fig. 2B). The treatments alone did not have significant effect on cell invasion compared with untreated non-irradiated cells, which is consistent with low HPSE1 expression in this cell line (Fig. S1). Irradiation jointly administered with anti-HPSE1 treatments maintained a constant reduction in cell invasion compared with the corresponding untreated irradiated cells. SCC-25 cells did not present the invasion-inducing effect seen in HSC-3 cells. Furthermore, in the SAS cell line irradiation alone also significantly decreased invasion dose-dependently (Fig. 2C). In addition, treatment with anti-HPSE1 and Erbitux significantly reduced the invasion of non-irradiated cells compared with untreated non-irradiated cells. In this case, treatment with anti-HPSE1 combined with irradiation of 4 Gy significantly decreased invasion compared with untreated irradiated cells. Altogether, IR and drug treatment seemed not to have synergic effects on invasion also in this cell line.

Ionizing radiation increases expression of MMPs and induces EMT in myoma model

IR has been shown to upregulate the amount of matrix metalloproteinases (MMPs) [6]. We therefore evaluated the effects of irradiation on MMP-2 and MMP-9 expression in HSC-3 cells by immunohistochemistry in a myoma model (Fig. 3A and B). We could see an increase in the number of HSC-3 cells positive for both MMP-2 and MMP-9 localized in the invasion area of myoma

samples irradiated with 8 Gy. In addition, IR may induce pro-survival signalling pathways, thereby enhancing cell proliferation [6]. In myoma discs, there were no significant changes in the levels of Ki-67 immunoreactivity in 2 Gy irradiated sections compared with non-irradiated ones, indicating no changes in cell proliferation (Fig. 4A and B). Furthermore, IR is known to induce epithelial-mesenchymal transition (EMT) in cells, and therefore, we also analysed common epithelial marker E-cadherin and mesenchymal marker vimentin [35] in irradiated myomas by immunohistochemistry (Fig. 4C-F). In addition, we analysed HPSE1, which usually increases with IR (Fig. 4G-J) [36]. Our analysis showed that the level of E-cadherin was significantly decreased (Fig. 4C and D) and vimentin increased in HSC-3 cells when myomas were irradiated with 2 Gy (Fig. 4E and F). The level of HPSE1 was increased in 2 Gy irradiated discs, while cells were counted both from the surface of the section and from the invasion area and compared with the total cell number (Fig. 4G-J). Our data suggest that low doses of IR may increase MMP and HPSE1 expression and initiate EMT in cells cultured in the myoma model.

HSC-3 cells, after irradiation and invasion, recover and do not present any additional changes in proliferation, clonogenic viability or further invasion capacity

To further determine the effects of irradiation and invasion on the HSC-3 cells, we established cell clones from previously 0, 2, 4 and 8 Gy irradiated cells, from the bottom of the Myogel Transwell invasion assay plates. To perform the assays, two clones were cultured over 4-10 passages, and cells in each experiment had an equal passage number. Proliferation and clonogenic viability of sub-cultured, previously irradiated and invaded cells were tested with BrdU and clonogenic assays. In these assays, the previously irradiated invaded cells had proliferation and clonogenic viability comparable to normal HSC-3 cells (Fig. 5A and B). We also conducted a Myogel Transwell invasion assay, in which no statistically significant difference was observed (Fig. 5C). Furthermore, we analysed phosphorylation of EGF receptor and its downstream signalling protein kinases Akt

and Erk1/2 of serum-starved and 1-h serum-treated cells by immunoblot (Fig. 5D). Previous irradiation and invasion did not induce phosphorylation of EGFR, Akt and Erk1/2 in HSC-3 cells, as there were no significant changes observed in the ratio of the phosphorylated form/total protein (Fig. 5D). Instead, there seemed to be a trend to lower phosphorylation of Akt and Erk1/2 with doses of 4 and 8 Gy compared with the HSC-3 control. Our data suggest that IR and invasion do not have long-term effects on proliferation, clonogenic viability, invasion and activation of signalling pathway proteins in HSC-3 cells.

Previous irradiation and invasion of HSC-3 cells results in upregulation of MMP-2 and MMP-9

As we saw changes in the amount of MMP-2 and MMP-9 staining in irradiated myomas, supporting the previous findings with IR and MMPs [5], [6], [35] we also studied these MMPs in clones of previously irradiated and invaded HSC-3 cells. We used zymography and EnzChek assay to evaluate the MMP amount and gelatinase activities in our previously irradiated and invaded HSC-3 cells, respectively. In zymography, conditioned media were separated on SDS-PAGE casted in the presence of fluorescently labelled gelatin, and the sample intensities were normalized to the cellular soluble protein concentration. On zymography gel, we could see bands corresponding to pro-MMP-9 and pro- and active-MMP-2 standards (Fig. 6A). Quantification of these bands showed that irradiation dose dependently increased the levels of pro-MMP-2 and -9, active-MMP-2 and the total level of these enzymes compared with control non-irradiated cells (Fig. 6B and C).

The overall gelatinase activity of the conditioned medium was assayed with the EnzChek® Gelatinase Assay Kit. The fluorescence intensities of samples were normalized to the cellular soluble protein concentration. The combined gelatin-digesting enzyme activity was not induced dose-dependently in irradiated invaded cells (Fig. 6D), suggesting that induction could be specific for MMP-2 and -9.

To assess EMT in clones of previously irradiated and invaded cells, we analysed E-cadherin and vimentin by immunoblots. In addition, we analysed the amount of HPSE1. The immunoblot analysis suggests that previous irradiation and invasion do not trigger EMT in HSC-3 cells, while the amounts of E-cadherin and vimentin were not significantly changed (Fig. 7A-B). Furthermore, the amount of HPSE1 was unchanged in clones of previously irradiated and invaded cells (Fig.7A and C).

Combination of ionizing radiation and anti-HPSE1 aptamers does not significantly alter the clonogenic viability of HSC-3 cells

We recently showed that 1.5 M short heparanase aptamer does not affect cell viability [25]. We wanted to further investigate how this treatment combined with irradiation affects OTSCC cells. Therefore, the effect of anti-HPSE1, 1.5 M short protected heparanase aptamer and Erbitux in combination with irradiation on the clonogenic viability of HSC-3 cell line was assessed with a clonogenic assay (Fig. 8). Increasing numbers of cells were seeded and exposed to different doses of irradiation combined with drug treatments. Cell colonies were counted after one-week incubation. Results are presented as surviving fraction compared with untreated non-irradiated HSC-3 cells. The treatments alone showed varying degrees of effectiveness. The anti-HPSE1 and short protected aptamer against HPSE1 alone showed minimal effect, in accordance with previously published data [25], whereas Erbitux alone had a diminishing effect of >50% of clonogenic viability, however this was not statistically significant. Irradiation alone reduced the cell survival in a dose-dependent increasing manner, as expected. Overall, the relative survival of HSC-3 treated and irradiated cells, compared with corresponding untreated irradiated cells, was at the same level. This suggests that there is no synergistic effect of treatments and irradiation on cell survival in the conditions used here. There might also be a slight induction in survival with irradiation at a dose of

4 Gy in each treatment group, which was also confirmed after 72 h in a BrdU assay (data not shown). Our data suggest that IR does not significantly improve the effectiveness of anti-HPSE1 antibody, 1.5 M short protected aptamer and Erbitux, nor do these have a synergistic effect on cell viability.

DISCUSSION

We have previously shown that anti-heparanase aptamers inhibit the invasion of a highly aggressive OTSCC cell line, HSC-3, in myoma organotypic culture [25]. In this study, we analysed the effect of ionizing radiation (IR) alone, and the combined effects of HPSE1 inhibitors and IR on HSC-3 cell proliferation and invasion. We further analysed the potential use of our human 3D myoma organotypic disc model [12], [13], [15] and a gelatinous leiomyoma matrix, Myogel [14], [15], in *in vitro* chemoradiation studies by comparing these two models. Finally, we analysed the long-term effect of radiation and invasion by studying the clones of previously irradiated and invaded HSC-3 cells collected from a Myogel Transwell model. Our studies presented a number of important findings with regard to the effect of IR on cell invasion, alone or combined with the use of aptamer or antibody-based HPSE1 inhibitors.

Treatment with both HPSE1 antibody and aptamer had an inhibiting effect on the invasion of non-irradiated HSC-3 cells in myoma discs and Myogel assays, confirming the accurateness of both invasion models. This is also consistent with our previous results showing that anti-HPSE1 and 1.5 M short aptamer significantly decreases the total invasion area and invasion depth of HSC-3 cells in myoma discs [25]. Our original premise was that IR induces HPSE1 expression [36], and this may lead to increased invasion capacity, which could be controlled using HPSE1 inhibitors. Our results with the myoma model confirmed increased expression of HPSE1, as well as MMP-2 and MMP-9

upon irradiation. However, in the invasion study, HPSE1 inhibitors were found to induce HSC-3 invasion when cells were irradiated with doses of 4 and 8 Gy. This suggests that there may be other pathways regulating invasion, which are induced due to HPSE1 blocking and subsequent irradiation. Additionally, it was recently shown that knockdown of HPSE might actually upregulate MMP-2 and MMP-9 expression [37], [38]. This would explain the increase in invasion of HPSE1 antibody or aptamer treated HSC-3 cells after irradiation found in this study. This is further supported by our control experiments using two other OTSCC cell lines, both low in heparanase expression, where use of anti-HPSE aptamer did not alter the profile of invasion relative to the irradiated, non-treated cells. Our data further suggest that our human 3D myoma organotypic model [12], [13] and a gelatinous leiomyoma matrix Myogel [14] are both appropriate for chemoradiation assays, and results with the tested set of drugs were consistent with both experiments.

As our HPSE1 inhibitor treatments and irradiation seemed to have a significant effect on the HSC-3 cell line, we further analysed the long-term effects of IR and invasion on this cell line. Therefore, we analysed cells in irradiated myomas and established irradiated and invaded cell clones from the Myogel invasion assay. IR is known to trigger several signal pathways with both pro- and anti-proliferative and migratory activities. Therefore, the cells that escape the lethal effects of IR may proliferate more and display enhanced invasive potential [5], [6], [39]. Our results showed that irradiation and invasion did not have at least long-term effects on proliferation, clonogenic viability and invasion of HSC-3 clones. Also in the myoma model, irradiated cells did not show increased proliferation or invasion. IR has been shown to promote the epidermal growth factor receptor (EGFR) homo- or heterodimerization that activates downstream pathways, such as mitogen-activated protein kinase (MAPK) cascade and phosphatidylinositol-4,5-bisphosphate 3-kinase (PI3K) signalling, which regulate growth, survival, proliferation and cell migration [6], [35], [40], [41]. Our immunoblot analysis of serum-starved and 1-h serum-treated cells showed that there were

no changes in activation of EGFR, Erk1/2 or Akt in irradiated and invaded cells. This finding is consistent with our proliferation, clonogenic viability and invasion assays, which also showed no significant differences.

In our immunohistochemical analysis, MMP-2 and MMP-9 amounts were induced after irradiation in the myoma model. Increased levels of MMP-2 and MMP-9 have been also previously described in irradiated cancer cells [5], [6], [35]. In several studies, the enhanced invasiveness of irradiated cancer cells has been linked to the increased activity of MMP-2 and MMP-9 [42]–[45]. In our analyses of irradiated HSC-3 cells in myoma at 8 Gy, we saw an increase in both MMP-2 and MMP-9. However, we could not observe induced invasion, at least not until 4 Gy, although this appeared to revert with a dose of 8 Gy. In clones of HSC-3 cells previously irradiated and invaded, the level of pro-MMP-2 and pro-MMP-9 and active-MMP-2 increased in a dose-dependent manner with the radiation previously received by the parent cells. However, this did not appear to induce activation of ERK and PI3K/Akt signalling pathways. According to Purushothaman and co-workers, elevated HPSE1 expression upregulates MMP-9 expression and this stimulation depends on the ERK signalling pathway [46]. On the other hand, IR has been suggested to regulate MMP-2 and MMP-9 expression through the PI3K/Akt signalling pathway [44], [45], and IR has been shown to increase HPSE1 expression in PANC-1 cells [36]. It is therefore possible that this is all part of the same pathway, where IR augments HPSE1 expression, which in turn regulates MMP-2 and MMP-9 expression. The HSC-3 cell line has been shown to have intense HPSE1 mRNA expression and enzyme activity [47], [48]. Indeed, our analysis of HPSE1-positive cells in the myoma model demonstrated an increase in HPSE1 expression during irradiation, as well as MMP-2 and MMP-9 expression, suggesting that HPSE1-mediated signalling of MMP-9 upregulation might be active in this model. Interestingly, although HPSE1 overexpression ceased in the clones of the previously irradiated and invading HSC-3 cells, these maintained increased MMP-2 and MMP-9 expression. It

453 is possible that MMP-2 and MMP-9 expression is turned on even if the signalling pathways are no
454 longer activated.
455
456 Epithelial-mesenchymal transition (EMT) is a process in which the normal epithelial cells gain pro-
457 invasive characteristics, such as loss of attachment to each other and to the basement membrane,
458 and gain enhanced motility [49]. IR has been shown to induce EMT [6], [35], [50], which is
459 characterized by a progressive loss of epithelial morphology and markers, such as E-cadherin, and
460 gain of mesenchymal markers like vimentin [51]. We have recently shown that the myoma
461 organotypic model initiates expression of vimentin in HSC-3 cells [12]. In this study, we report that
462 IR further induces EMT in the myoma model, but loss of E-cadherin and appearance of vimentin
463 were not seen when the previously irradiated invading cells were subsequently cultured on plastic.
464 This could highlight the relevance of the environment, as plastic does not offer a realistic
465 surrounding for the cancer cells. The myoma model provides a more genuine, 3D environment in
466 which the cancer cells are in contact not only with each other but also with the surrounding matrix.
467
468 Finally, we analysed the clonogenic viability of the cells in the presence of HPSE1 inhibitors and
469 increasing doses of IR. In accordance with our previously published data, anti-HPSE aptamer has
470 little or no effect on cell viability, confirming that any observed inhibitory effects on invasion are
471 due to HPSE1 inhibition and not due to a cytotoxic effect. Furthermore, we labelled the 1.5 short
472 protected aptamer with 5' Alexa Fluor 546 label and followed them in a fluorescence microscopy
473 experiment, where we saw that the aptamer was taken successfully into the cells (unpublished data).
474 We found no significant difference between the use of IR alone and in combination with HPSE1
475 inhibitors, with perhaps a small exception regarding increased clonogenic viability at 4 Gy. The
476 most interesting finding is the inverse correlation observed between survival and invasiveness,
477 expressed mainly in cells treated with HPSE1 inhibitors and irradiated at 8 Gy. While at 8 Gy, only

a fraction of the cells remain alive (Fig. 8), there is an increased invasive activity associated with this population at this dose of irradiation (Figs 1A and 2A). This result might suggest, in fact, that there is a phenotype change in survivors after HPSE1 inhibitor treatment and irradiation that exacerbates the invasion capacity of these cells.

Conclusions

We found that human uterine leiomyoma-based ECM models, myoma discs and Myogel, are reliable methods for testing the effects of chemoradiation treatment on human carcinoma cells. Our data suggest that blocking of HPSE1 activity combined with IR may induce cell invasion. In addition, we showed that irradiation had a lasting effect on induction of MMP-2 and MMP-9.

ACKNOWLEDGEMENTS

We gratefully acknowledge Maija-Leena Lehtonen, Tanja Kuusisto, Eeva-Maija Kiljander, Piia Mäkelä and the staff of the Radiotherapy Unit of Oulu University Hospital for expert technical assistance. Paula Pesonen and Jari Jokelainen are thanked for assistance with statistical analyses. The work was supported by research grants from Sigrid Juselius Foundation, Cancer Foundation of Finland, Medical Research Center Oulu, Finnish Dental Society Apollonia, Orion Research Foundation, Ida Montin Foundation and research funds from the Medical Faculty of the University of Oulu and Oulu University Hospital special state support for research.

CONFLICT OF INTEREST

The authors have no potential conflicts of interest with respect to authorship and/or publication of this article.

REFERENCES

[1] N. S. Hillbertz, J.-M. Hirsch, J. Jalouli, M. M. Jalouli, and L. Sand, “Viral and molecular

aspects of oral cancer.," *Anticancer Res.*, vol. 32, no. 10, pp. 4201–12, Oct. 2012.

[2] C. Piazza, N. Montalto, A. Paderno, V. Taglietti, and P. Nicolai, "Is it time to incorporate 'depth of infiltration' in the T staging of oral tongue and floor of mouth cancer?," *Curr. Opin. Otolaryngol. Head Neck Surg.*, vol. 22, no. 2, pp. 81–89, Apr. 2014.

[3] J. A. Regezi, J. J. Sciubba, and R. C. K. Jordan, "Oral Pathology: Clinical Pathologic Correlations," in *Oral Pathology: Clinical Pathologic Correlations: Seventh Edition*, 2017, pp. 176–178.

[4] R. Mroueh *et al.*, "Improved outcomes with oral tongue squamous cell carcinoma in Finland," *Head Neck*, vol. 39, no. 7, pp. 1306–1312, Jul. 2017.

[5] C. Moncharmont *et al.*, "Radiation-enhanced cell migration/invasion process: A review," *Crit. Rev. Oncol. Hematol.*, vol. 92, no. 2, pp. 133–142, Nov. 2014.

[6] O. Kargiotis, A. Geka, J. S. Rao, and A. P. Kyritsis, "Effects of irradiation on tumor cell survival, invasion and angiogenesis," *J. Neurooncol.*, vol. 100, no. 3, pp. 323–338, Dec. 2010.

[7] S. K. Kundu and M. Nestor, "Targeted therapy in head and neck cancer," *Tumor Biol.*, vol. 33, no. 3, pp. 707–721, Jun. 2012.

[8] A. G. Sacco and E. E. Cohen, "Current Treatment Options for Recurrent or Metastatic Head and Neck Squamous Cell Carcinoma," *J. Clin. Oncol.*, vol. 33, no. 29, pp. 3305–3313, Oct. 2015.

[9] J. B. Vermorken and P. Specenier, "Optimal treatment for recurrent/metastatic head and neck cancer," *Ann. Oncol.*, vol. 21, no. Supplement 7, pp. vii252-vii261, Oct. 2010.

[10] A. Argiris *et al.*, "Evidence-Based Treatment Options in Recurrent and/or Metastatic Squamous Cell Carcinoma of the Head and Neck," *Front. Oncol.*, vol. 7, no. 72, May 2017.

[11] P. Szturz and J. B. Vermorken, "Immunotherapy in head and neck cancer: aiming at EXTREME precision," *BMC Med.*, vol. 15, no. 1, p. 110, Dec. 2017.

528 [12] S. Nurmenniemi *et al.*, "A Novel Organotypic Model Mimics the Tumor
529 Microenvironment," *Am. J. Pathol.*, vol. 175, no. 3, pp. 1281–1291, Sep. 2009.
530 [13] P. Åström, R. Heljasvaara, P. Nyberg, A. Al-Samadi, and T. Salo, "Human Tumor Tissue-
531 Based 3D In Vitro Invasion Assays," in *Methods in Molecular Biology*, vol. 1731, 2018, pp.
532 213–221.
533 [14] T. Salo *et al.*, "A novel human leiomyoma tissue derived matrix for cell culture studies,"
534 *BMC Cancer*, vol. 15, no. 1, p. 981, Dec. 2015.
535 [15] T. Salo *et al.*, "Organotypic three-dimensional assays based on human leiomyoma–derived
536 matrices," *Philos. Trans. R. Soc. B Biol. Sci.*, vol. 373, no. 1737, p. 20160482, 2018.
537 [16] S. Teppo *et al.*, "The hypoxic tumor microenvironment regulates invasion of aggressive oral
538 carcinoma cells," *Exp. Cell Res.*, vol. 319, no. 4, pp. 376–389, Feb. 2013.
539 [17] E. Sundquist *et al.*, "Neoplastic extracellular matrix environment promotes cancer invasion in
540 vitro," *Exp. Cell Res.*, vol. 344, no. 2, pp. 229–240, Jun. 2016.
541 [18] A. R. Chin and S. E. Wang, "Cancer Tills the Premetastatic Field: Mechanistic Basis and
542 Clinical Implications," *Clin. Cancer Res.*, vol. 22, no. 15, pp. 3725–3733, Aug. 2016.
543 [19] J. Sceneay, M. J. Smyth, and A. Möller, "The pre-metastatic niche: finding common
544 ground," *Cancer Metastasis Rev.*, vol. 32, no. 3–4, pp. 449–464, Dec. 2013.
545 [20] S. S. McAllister and R. A. Weinberg, "The tumour-induced systemic environment as a
546 critical regulator of cancer progression and metastasis," *Nat. Cell Biol.*, vol. 16, no. 8, pp.
547 717–727, Aug. 2014.
548 [21] R. N. Kaplan *et al.*, "VEGFR1-positive haematopoietic bone marrow progenitors initiate the
549 pre-metastatic niche," *Nature*, vol. 438, no. 7069, pp. 820–827, Dec. 2005.
550 [22] H. K. Eltzschig and P. Carmeliet, "Hypoxia and Inflammation," *N. Engl. J. Med.*, vol. 364,
551 no. 7, pp. 656–665, Feb. 2011.
552 [23] B. Psaila and D. Lyden, "The metastatic niche: adapting the foreign soil," *Nat. Rev. Cancer*,

vol. 9, no. 4, pp. 285–293, Apr. 2009.

[24] J. P. Sleeman, “The metastatic niche and stromal progression,” *Cancer Metastasis Rev.*, vol. 31, no. 3–4, pp. 429–440, Dec. 2012.

[25] S. C. Simmons *et al.*, “Anti-Heparanase Aptamers as Potential Diagnostic and Therapeutic Agents for Oral Cancer,” *PLoS One*, vol. 9, no. 10, p. e96846, Oct. 2014.

[26] X. He, P. E. C. Brenchley, G. C. Jayson, L. Hampson, J. Davies, and I. N. Hampson, “Hypoxia Increases Heparanase-Dependent Tumor Cell Invasion, Which Can Be Inhibited by Antiheparanase Antibodies,” *Cancer Res.*, vol. 64, no. 11, pp. 3928–3933, Jun. 2004.

[27] F. Worden and A. G. Sacco, “Molecularly targeted therapy for the treatment of head and neck cancer: a review of the ErbB family inhibitors,” *Onco. Targets. Ther.*, vol. 9, p. 1927, Apr. 2016.

[28] S. C. Simmons *et al.*, “Development of Novel Single-Stranded Nucleic Acid Aptamers against the Pro-Angiogenic and Metastatic Enzyme Heparanase (HPSE1),” *PLoS One*, vol. 7, no. 6, p. e37938, Jun. 2012.

[29] N. A. P. Franken, H. M. Rodermond, J. Stap, J. Haveman, and C. van Bree, “Clonogenic assay of cells in vitro,” *Nat. Protoc.*, vol. 1, no. 5, pp. 2315–2319, Dec. 2006.

[30] P. Nyberg *et al.*, “Endostatin Inhibits Human Tongue Carcinoma Cell Invasion and Intravasation and Blocks the Activation of Matrix Metalloprotease-2, -9, and -13,” *J. Biol. Chem.*, vol. 278, no. 25, pp. 22404–22411, Jun. 2003.

[31] F. Momose, T. Araida, A. Negishi, H. Ichijo, S. Shioda, and S. Sasaki, “Variant sublines with different metastatic potentials selected in nude mice from human oral squamous cell carcinomas,” *J. Oral Pathol. Med.*, vol. 18, no. 7, pp. 391–395, Aug. 1989.

[32] K. Matsumoto, K. Matsumoto, T. Nakamura, and R. H. Kramer, “Hepatocyte growth factor/scatter factor induces tyrosine phosphorylation of focal adhesion kinase (p125FAK) and promotes migration and invasion by oral squamous cell carcinoma cells.,” *J. Biol.*

578 *Chem.*, vol. 269, no. 50, pp. 31807–13, Dec. 1994.
579 [33] D. M. Ramos *et al.*, "Stromal fibroblasts influence oral squamous-cell carcinoma cell
580 interactions with tenascin-C.," *Int. J. cancer*, vol. 72, no. 2, pp. 369–76, Jul. 1997.
581 [34] K. Okumura, A. Konishi, M. Tanaka, M. Kanazawa, K. Kogawa, and Y. Niitsu,
582 "Establishment of high- and low-invasion clones derived for a human tongue squamous-cell
583 carcinoma cell line SAS.," *J. Cancer Res. Clin. Oncol.*, vol. 122, no. 4, pp. 243–8, 1996.
584 [35] S. Y. Lee *et al.*, "Induction of metastasis, cancer stem cell phenotype, and oncogenic
585 metabolism in cancer cells by ionizing radiation," *Mol. Cancer*, vol. 16, no. 1, p. 10, Dec.
586 2017.
587 [36] A. Meirovitz *et al.*, "Role of Heparanase in Radiation-Enhanced Invasiveness of Pancreatic
588 Carcinoma," *Cancer Res.*, vol. 71, no. 7, pp. 2772–2780, Apr. 2011.
589 [37] Y. Yang *et al.*, "Nuclear heparanase-1 activity suppresses melanoma progression via its
590 DNA-binding affinity," *Oncogene*, vol. 34, no. 47, pp. 5832–5842, Nov. 2015.
591 [38] E. Zcharia *et al.*, "Newly Generated Heparanase Knock-Out Mice Unravel Co-Regulation of
592 Heparanase and Matrix Metalloproteinases," *PLoS One*, vol. 4, no. 4, p. e5181, Apr. 2009.
593 [39] I. Madani, W. De Neve, and M. Mareel, "Does ionizing radiation stimulate cancer invasion
594 and metastasis?," *Bull. Cancer*, vol. 95, no. 3, pp. 292–300, Mar. 2008.
595 [40] M. Toulany, M. Minjgee, R. Kehlbach, J. Chen, M. Baumann, and H. P. Rodemann, "ErbB2
596 expression through heterodimerization with erbB1 is necessary for ionizing radiation- but not
597 EGF-induced activation of Akt survival pathway," *Radiother. Oncol.*, vol. 97, no. 2, pp. 338–
598 345, Nov. 2010.
599 [41] J. Bussink, A. J. van der Kogel, and J. H. Kaanders, "Activation of the PI3-K/AKT pathway
600 and implications for radioresistance mechanisms in head and neck cancer," *Lancet Oncol.*,
601 vol. 9, no. 3, pp. 288–296, Mar. 2008.
602 [42] A. Kaliski *et al.*, "Angiogenesis and tumor growth inhibition by a matrix metalloproteinase

603 inhibitor targeting radiation-induced invasion," *Mol. Cancer Ther.*, vol. 4, no. 11, pp. 1717–
604 1728, Nov. 2005.
605 [43] C. Wild-Bode, M. Weller, A. Rimner, J. Dichgans, and W. Wick, "Sublethal irradiation
606 promotes migration and invasiveness of glioma cells: implications for radiotherapy of human
607 glioblastoma.," *Cancer Res.*, vol. 61, no. 6, pp. 2744–50, Mar. 2001.
608 [44] C.-M. Park *et al.*, "Ionizing Radiation Enhances Matrix Metalloproteinase-2 Secretion and
609 Invasion of Glioma Cells through Src/Epidermal Growth Factor Receptor–Mediated p38/Akt
610 and Phosphatidylinositol 3-Kinase/Akt Signaling Pathways," *Cancer Res.*, vol. 66, no. 17,
611 pp. 8511–8519, Sep. 2006.
612 [45] J. C.-H. Cheng, C. H. Chou, M. L. Kuo, and C.-Y. Hsieh, "Radiation-enhanced
613 hepatocellular carcinoma cell invasion with MMP-9 expression through PI3K/Akt/NF-κB
614 signal transduction pathway," *Oncogene*, vol. 25, no. 53, pp. 7009–7018, Nov. 2006.
615 [46] A. Purushothaman, L. Chen, Y. Yang, and R. D. Sanderson, "Heparanase Stimulation of
616 Protease Expression Implicates It as a Master Regulator of the Aggressive Tumor Phenotype
617 in Myeloma," *J. Biol. Chem.*, vol. 283, no. 47, pp. 32628–32636, Nov. 2008.
618 [47] H. Kurokawa *et al.*, "Heparanase and tumor invasion patterns in human oral squamous cell
619 carcinoma xenografts," *Cancer Sci.*, vol. 94, no. 3, pp. 277–285, Mar. 2003.
620 [48] M. Ikuta, K. A. Podyma, K. Maruyama, S. Enomoto, and M. Yanagishita, "Expression of
621 heparanase in oral cancer cell lines and oral cancer tissues," *Oral Oncol.*, vol. 37, no. 2, pp.
622 177–184, Feb. 2001.
623 [49] D. C. Radisky and M. A. LaBarge, "Epithelial-Mesenchymal Transition and the Stem Cell
624 Phenotype," *Cell Stem Cell*, vol. 2, no. 6, pp. 511–512, Jun. 2008.
625 [50] S. Lamouille, J. Xu, and R. Derynck, "Molecular mechanisms of epithelial–mesenchymal
626 transition," *Nat. Rev. Mol. Cell Biol.*, vol. 15, no. 3, pp. 178–196, Mar. 2014.
627 [51] C. Chen *et al.*, "Evidence for Epithelial-Mesenchymal Transition in Cancer Stem Cells of

Head and Neck Squamous Cell Carcinoma," *PLoS One*, vol. 6, no. 1, p. e16466, Jan. 2011.

FIGURE LEGENDS

Figure 1. Organotypic culture of drug-treated and irradiated HSC-3 cells. HSC-3 cell invasion in myoma discs at day 18 was analysed after treatment with 10 µg/ml of an antibody against heparanase (Anti-HPSE1) and 1 µM 1.5 M short protected heparanase aptamer and irradiation with doses of 0, 2, 4 and 8 Gy at day 12. The invasion area (A) and invasion depth (B) were measured from the pancytokeratin-stained histological sections (n=24/treatment) with Fiji software. P-values were calculated using independent samples #= Student´s T-test, *= Mann-Whitney U-test or ¶=Wilcoxon non-parametric signed-rank test. One symbol $p<0.05$, Two symbols $p<0.01$, Three symbols $p<0.001$.

Figure 2. Transwell invasion assay of drug-treated and irradiated OTSCC cell lines. HSC-3 (A), SCC-25 (B) and SAS (C) cell invasion in Myogel coated Transwells was analysed after treatment with 10 µg/ml of an antibody against heparanase (Anti-HPSE1), 1 µM 1.5 M short protected heparanase aptamer and 10 µg/ ml of Erbitux and irradiation with doses of 0, 2, 4 and 8 Gy. The invaded cells were stained with Toluidine Blue, the stain was dissolved in 1% SDS solution and the absorbance at 650 nm was measured. The values represent the average ± SD of three to five separate experiments. P-values were calculated using Mann-Whitney U-test. * $p<0.05$, ** $p<0.01$, *** $p<0.001$.

Figure 3. Immunostaining of MMP-2 and MMP-9 in HSC-3 cells in irradiated organotypic culture. HSC-3 cells were cultured on top of myoma discs and irradiated with doses of 0 and 8 Gy at day 12. The day 18 paraffin-embedded sections were immunostained with MMP-2 (A) and MMP-9 (B) antibodies. Scale bar 200 µm.

Figure 4. Immunostaining of Ki-67, EMT markers and HPSE1 in HSC-3 cells in irradiated organotypic culture. HSC-3 cells were cultured on top of myoma discs and irradiated with doses of 0 and 2 Gy at day 12. The day 18 paraffin-embedded sections were immunostained with the proliferation marker Ki-67 (A), epithelial marker E-cadherin (C), the mesenchymal marker vimentin (E) and heparanase (HPSE1) (G) antibodies. Cell proliferation rate was quantified (n=6 fields) as a percentage of Ki-67-positive carcinoma cells among all carcinoma cells per microscopic field at 200 x magnification (B). With E-cadherin, the intensity of staining was scored both from the surface area and invasion area (n=6 fields) (D). For vimentin (F) and HPSE1 (H-J), the scoring was assessed by counting the percentage of positive cells/total cells with 400 x magnification (n=6 fields). P-values were calculated using Mann-Whitney U-test. * $p<0.05$, ** $p<0.01$, *** $p<0.001$.

Figure 5. Analysis of previously irradiated and invaded HSC-3 cells. The irradiated invaded cells had proliferation (A) and clonogenic viability (B) comparable to normal HSC-3 cells while tested with BrdU and clonogenic assay, respectively. Irradiation and invasion did not significantly induce invasion of HSC-3 cells in Myogel Transwell invasion assay (C). The values (A-C) represent the average ± SD of three to five separate experiments. In immunoblot analysis (30 µg of soluble protein), irradiation and invasion seemed not to induce phosphorylation of EGFR, Akt and Erk1/2 in HSC-3, as there were no significant changes in the ratio of phosphorylated form/total protein band (D). The results represent the average of two independent experiments, separated twice on SDS-PAGE gels**.** In Figure D, representative immunoblots are shown.

Figure 6. Zymography and gelatinase assays of irradiated and invaded HSC-3 cells. In gel zymography the conditioned concentrated media of normal and irradiated and invaded HSC-3 cells were separated on SDS-PAGE. The acrylamide gel was embedded with fluorescently labelled

gelatin (A). Purified gelatinase standards are shown on the right: pro-MMP-2 (72 kDa), active MMP-2 (62 kDa), pro-MMP-9 (92 kDa) and active MMP-9 (82 kDa). In Figure A, a representative zymography gel is shown. The amount of proMMP-2 and -9, active MMP-2 (B) and total amount of these MMPs (C) in zymography gels was quantified with Fiji software, and intensities were normalized to the cellular soluble protein concentration. The overall gelatinase activity of conditioned medium was assayed with EnzChek® Gelatinase Assay Kit (D). The fluorescence intensities were normalized to the cellular soluble protein concentration. The results represent the average ± SD of three separate sample sets each analysed three to four times. P-values were calculated using Mann-Whitney U-test. * $p<0.05$, ** $p<0.01$, *** $p<0.001$.

Figure 7. Immunoblot analysis of EMT markers and HPSE1 in irradiated and invaded HSC-3 cells. Normal and irradiated and invaded HSC-3 cell homogenates (50 µg of soluble protein) were separated on SDS-PAGE gels. Amounts of epithelial marker E-cadherin, the mesenchymal marker vimentin and heparanase (HPSE1) were analysed with immunoblots (A). In Figure A, representative immunoblots are shown. Beta-actin was used as a control to normalize the quantities of E-cadherin (B), vimentin (C) and HPSE1 (D). The results represent average ± SD of four independent experiments, separated three times on SDS-PAGE gels.

Figure 8. Clonogenic viability of drug treated and irradiated HSC-3 cell line. Cells were treated with 10 µg/ml of an antibody against heparanase (Anti-HPSE1), 1 µM 1.5 M short protected heparanase aptamer and 10 µg/ ml of Erbitux and irradiated with doses of 0, 2, 4 or 8 Gy. Cell colonies were cultured 7 days, fixed and stained with crystal violet (A). In figure A, representative 24-wells irradiated with 0 and 8 Gy are shown. The clonogenic viability was presented as the surviving fraction relative to untreated non-irradiated HSC-3 cells (B). The results represent the average of three separate experiments.

Figure 1

Click here to download high resolution image

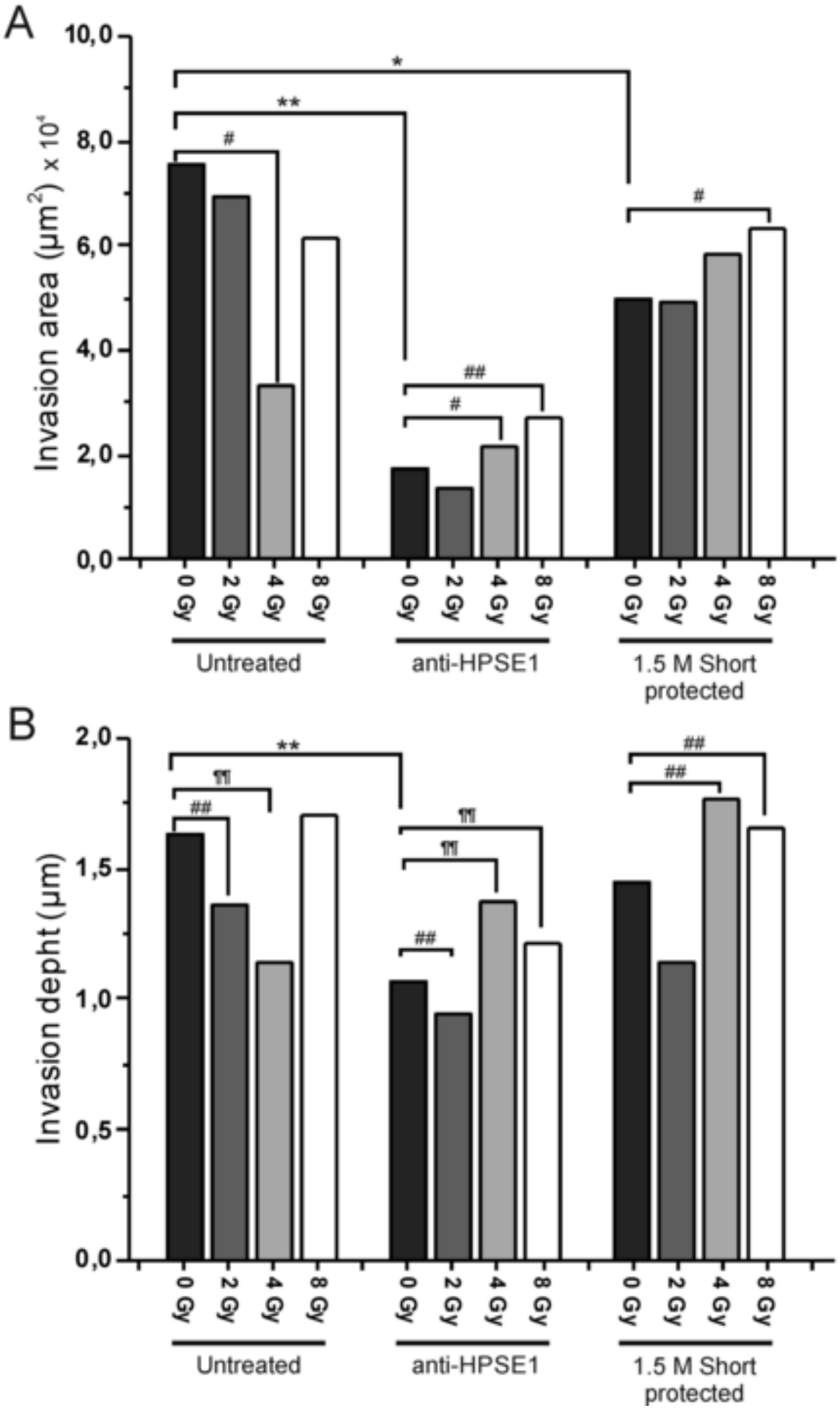

Figure 2

Click here to download high resolution image

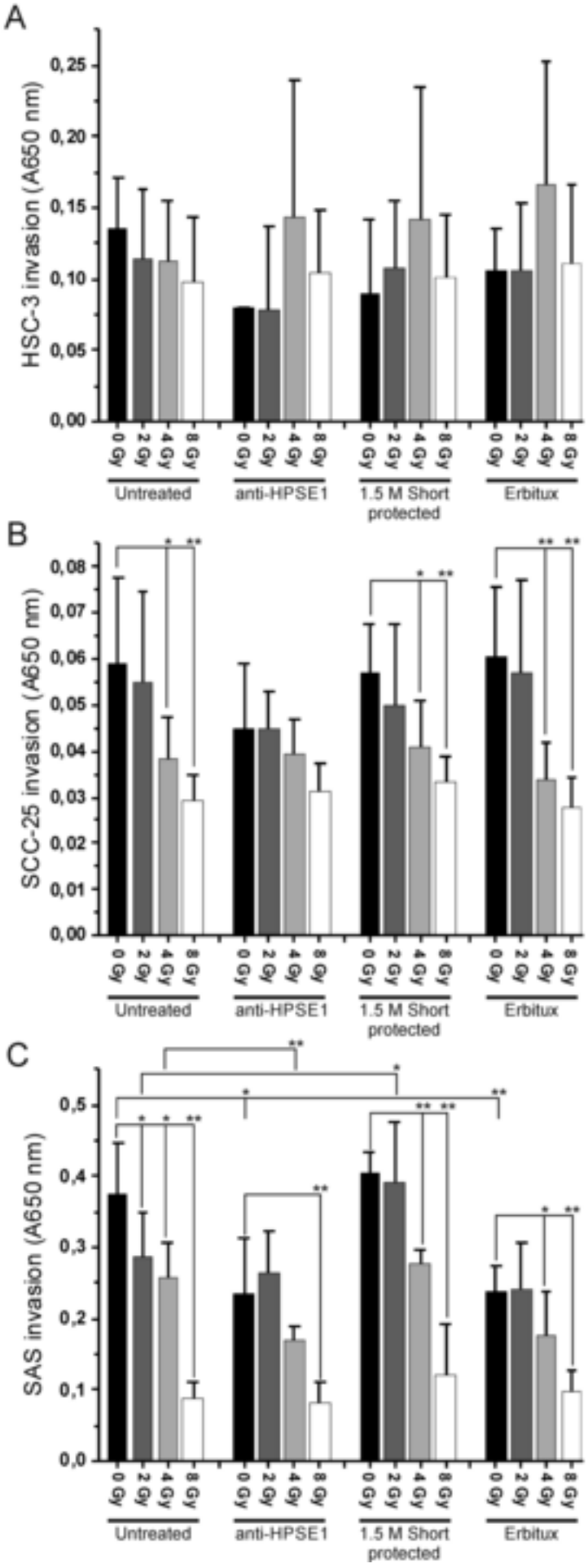

Figure 3

Click here to download high resolution image

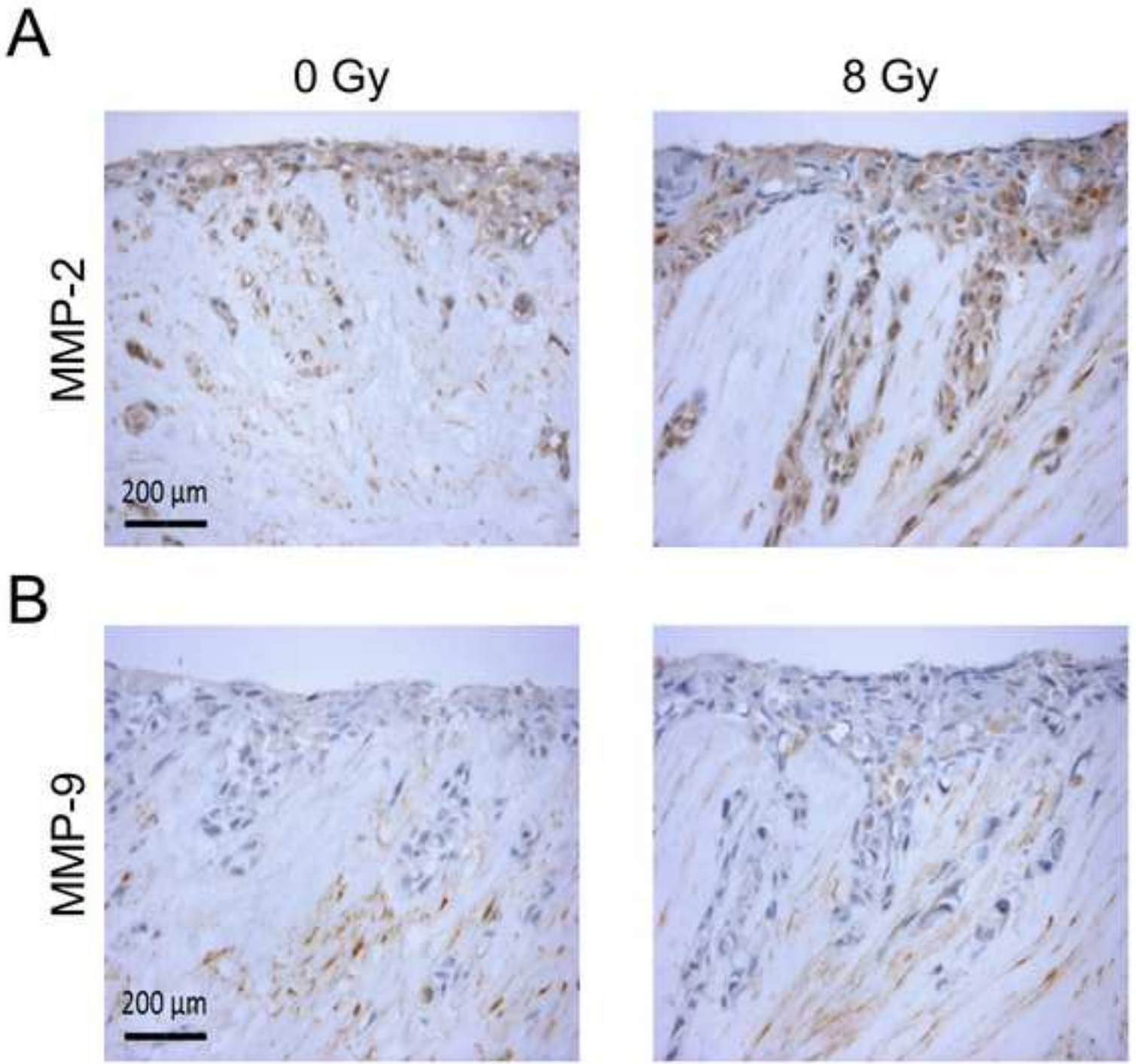

Figure 4

Click here to download high resolution image

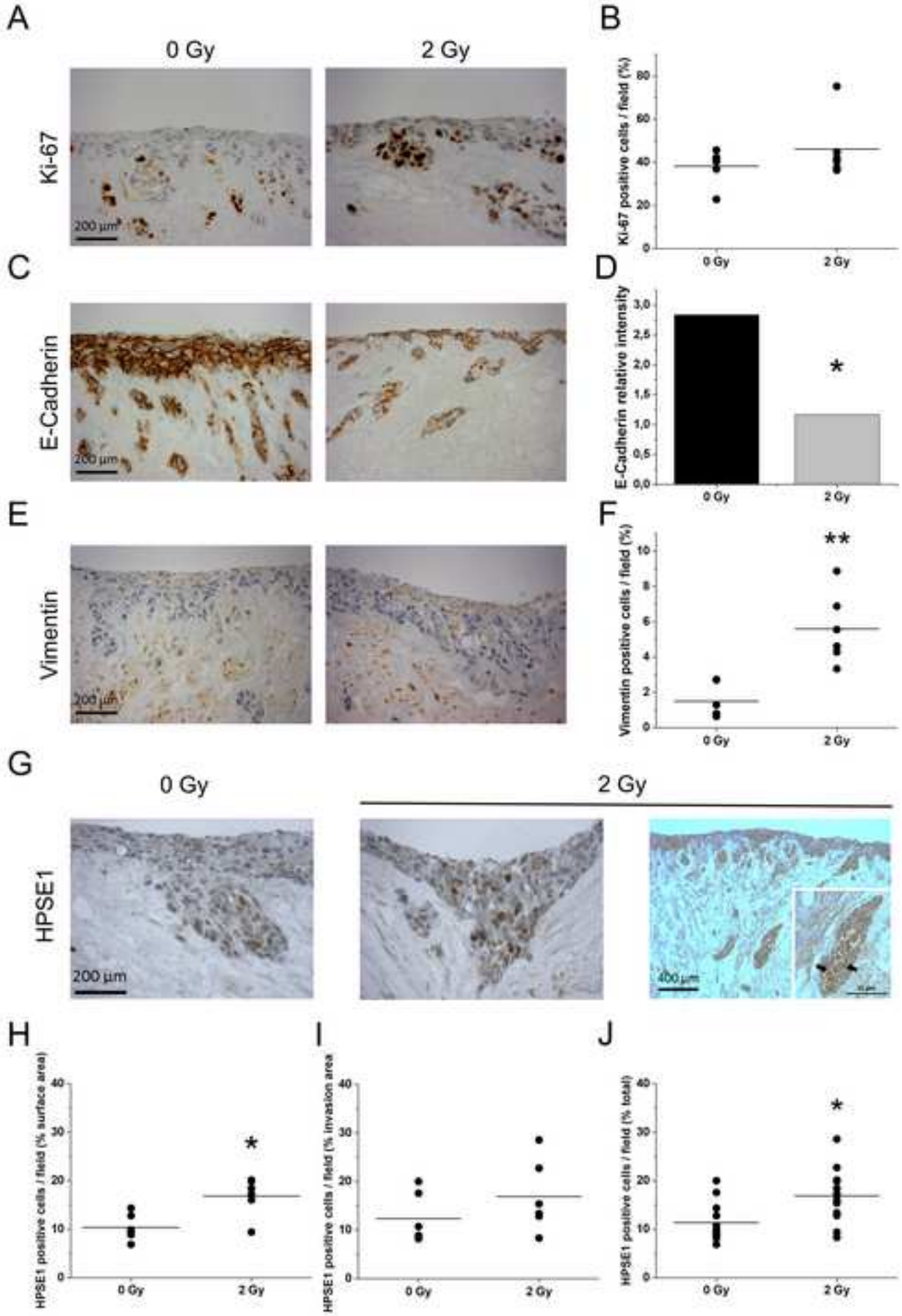

Figure 5

Click here to download high resolution image

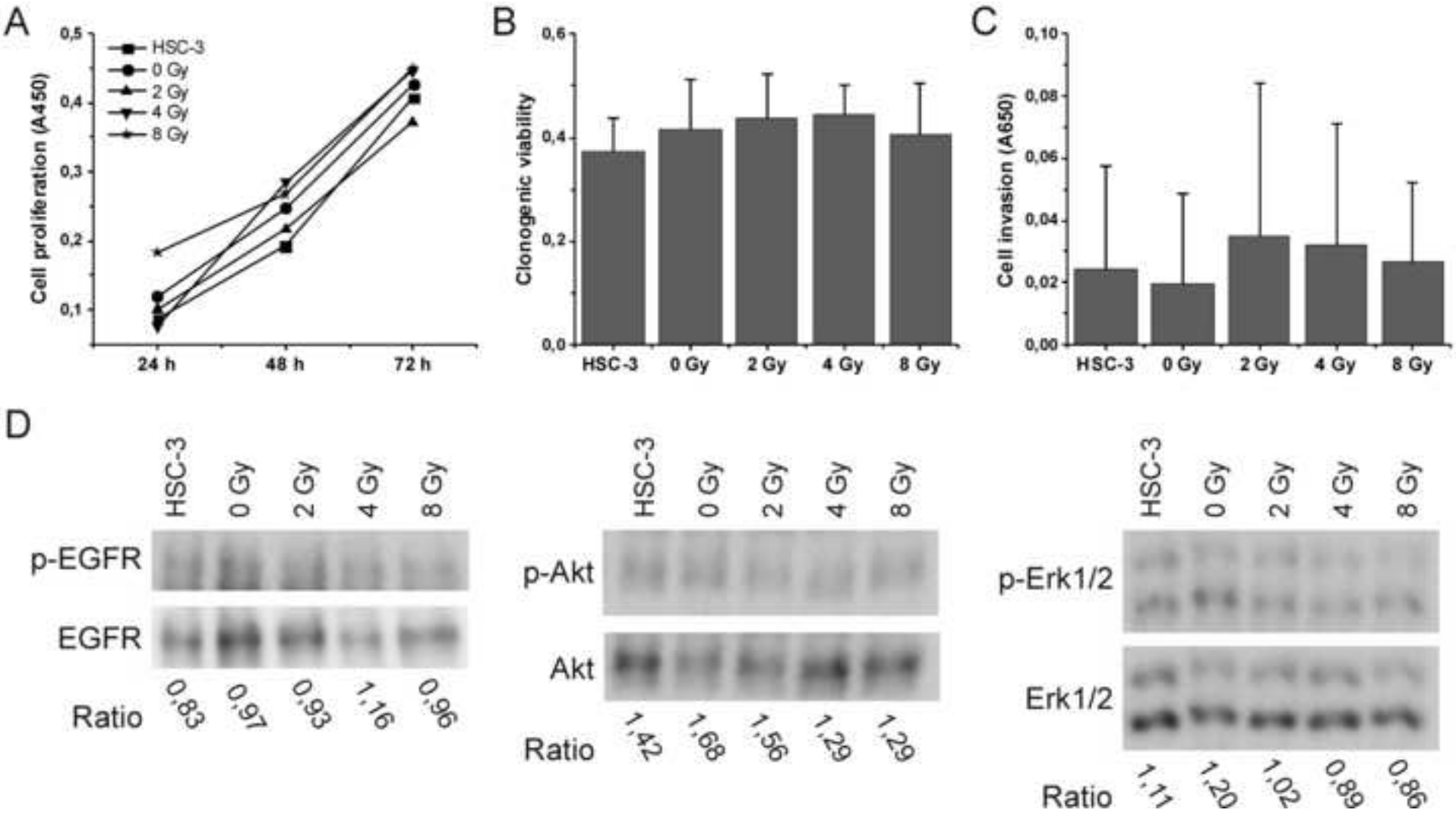

Figure 6

Click here to download high resolution image

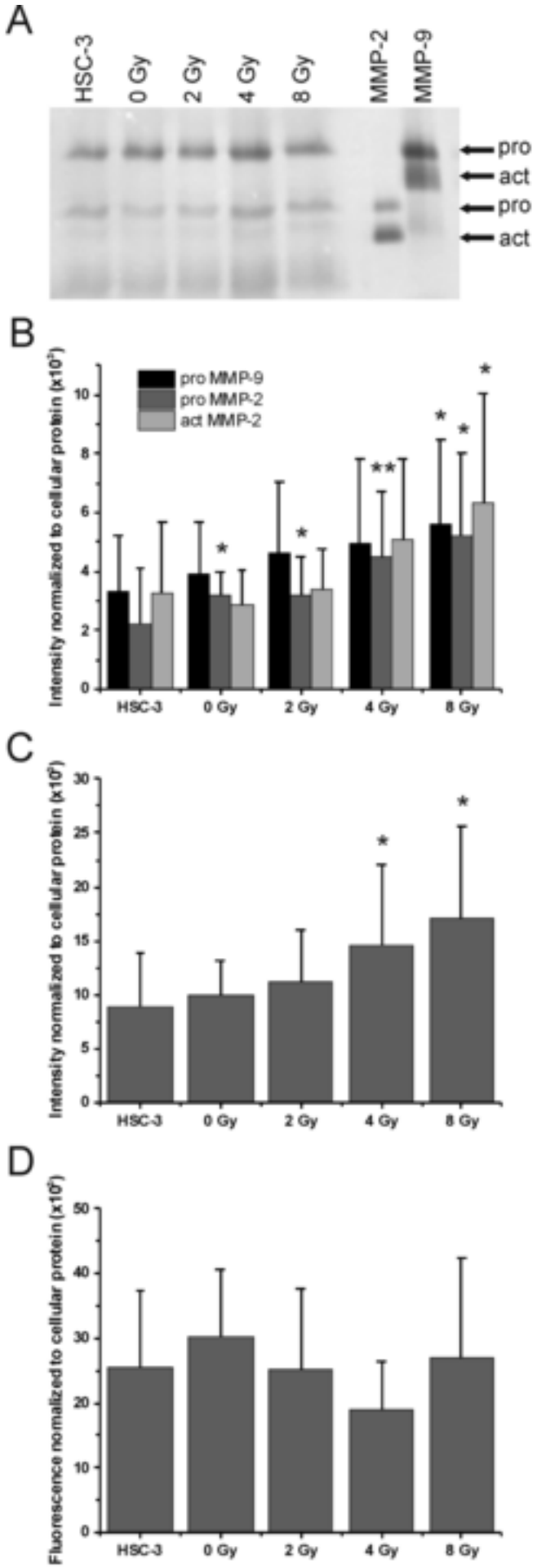

Figure 7

Click here to download high resolution image

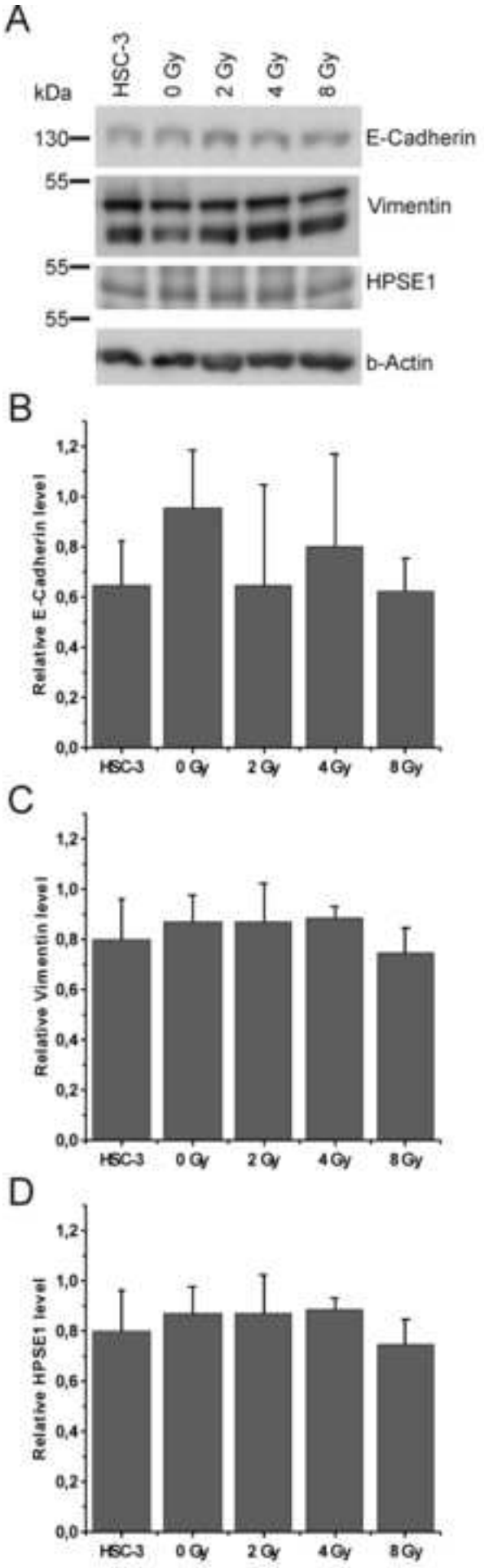

Figure 8

Click here to download high resolution image